THE MAGNETIC PROPERTIES OF THE QUATERNARY INTERMETALLIC COMPOUNDS $GdNi_2B_2C$

B.Giordanengo,M.El Massalami, S.L.Bud'ko and E.M.Baggio-Saitovitch.

CBPF, R.Xavier Sigaud 150, 22290-180, Rio de Janeiro, Brazil

J.Voiron

Lab. Louis-Neel, CNRS, Grenoble Cedex 09

A.Sulpice

CRTBT,CNRS,BP 166,38042 Grenoble Cedex 09

ABSTRACT

Magnetization studies on $GdNi_2B_2C$, over a wide temperature and field ranges, reveal two magnetic phase transitions at 19.5(5) K and at 7.2(3)K. At T=1.7K, the full Gd-moment saturation is attained only for $H \geq H_c$=133(3) kOe. The overall magnetic features are similar to the magnetic properties of the RNi_2B_2C (R= Tm, Er, Ho, Dy, Tb) isomorphs and can be interpreted in terms of the picture that assumes the weakly-anisotropic Gd-moments to be RKKY-coupled ferromagnetically in plane and antiferromagnetically out-of-plane.

Keywords: $GdNi_2B_2C$, weak-anisotropy, magnetic interactions.

1. INTRODUCTION

The intermetallic antiferromagnetic conductor $GdNi_2B_2C$ belongs to the family of compounds RNi_2B_2C (R=Y, rare earth) [1-4] that possess a body centered tetragonal structure with space group I4/mmm. The structure (which is a filled variant on the $ThCr_2Si_2$ structure) contains an alternate stacking of the Ni_2B_2 and the GdC sheets [2]. In the isomorphous intermetallics RNi_2B_2C (R=Tm, Er, Ho, Dy, Tb) [3-16], the 4f-moments have strong ferromagnetic (FM) intraplanar couplings and relatively weak antiferromagnetic (AFM) interplanar interactions: the paramagnetic Curie-Weiss temperature θ is positive [3,4] and for $T < T_N$ the spin structure is a set of FM planes that are AFM coupled [3-15].

Specific to the reentrant superconductor $HoNi_2B_2C$, the combined effects of these characteristic RKKY interactions and the easy plane crystal field anisotropy [16] lead to a unique helical spin arrangement. This state is energetically unstable at lower temperature and consequently transforms into a commensurate antiferromagnetic state at T_2[5,6,12,16]. The magnetic field influence on this helical state results in a characteristic H-T phase diagram [13-14,16].

On the other hand, for the case of the $GdNi_2B_2C$ compound [8,9,14,15], the spherical ^8S Gd-ions occupy the 4d sites (Wyckoff notation) with point symmetry operation 4/mmm [2]. Then, for $T > 1K$, the crystal field influences and the dipolar effects are expected to be negligible and so the anisotropic field $H_a \approx 0$. This weak-anisotropy (absence of complication due to crystal field effects) makes the $GdNi_2B_2C$ compound the best candidate in this series for studying the influence of the above

mentioned magnetic interactions on the low-T superconducting and magnetic properties.

2. RESULTS

The $GdNi_2B_2C$ compound was prepared by conventional argon arc-melting methods and was annealed as prescribed in the literature [2-4]. The room temperature Cu-Kα X-ray diffractogram (Fig.1) pertains to the required phase. Traces of impurities were detected, one of which was identified as GdNiBC[2]. The Rietveld profile analysis yields the same structural parameters as reported in Ref.[2]: a = 3.577Å and c = 10.36Å.

Magnetization measurements were carried out on the following standard set-ups: ac susceptibility (500Hz, 1 Oe, 1.5<T<50K), SQUID magnetometer (1.7K<T<100K, H<80 kOe) and extraction magnetometer (1.7K<T<100K, 0<H <140 kOe). Preliminary results on this compound were reported in Ref[8]. For T > 50K, the Curie-Weiss-type (C-W) Gd-paramagnetism is characterized by $\mu_{eff} = 7.97\mu_B$ and $\theta = +2.7$K. The positive θ indicates dominant intraplanar FM interactions. As the temperature decreases, a set of magnetic transitions appears (Fig.2). A weak peak around 40K is attributed to an unidentified magnetic impurity. The other two transitions (Fig.2) are intrinsic to the $GdNi_2B_2C$ compound [8]. One transition (peaking around $T_N=T_1$ = 19.5(5) K) is attributed to an AFM transition. Although, there is no experimental evidence on the existence of a helical state below T_N, however our experimental features can be qualitatively interpreted if we assume (in analogy with the magnetic feature of $HoNi_2B_2C$) an accompanying helical state that transforms to a commensurate AFM state at the second phase transition that occurs at $T_2 = 7.2(3)$ K.

Below T_1, the Field Cooled (FC) and Zero-Field Cooled (ZFC) magnetization curves (Fig.2) show that, a fraction of the magnetization is remnant under a 10 Oe magnetic field. This may be attributed to the combined effects of a strong planar ferromagnetism and a low anisotropic character.

Fig.3 shows the magnetization isotherms at T=2K, 9.76K, 24.23K, 33.84K, 48.16K, 76.56K. In the paramagnetic state, $T > \theta$ and the magnetization versus H/T curves should collapse to :

$$M = \chi H = CH/(T+\theta) \approx CH/T \propto H/T \quad (1)$$

This is confirmed in Fig.3.a, where <..> denotes the thermally averaged value (g is the g-factor and J is total orbital moment). In addition, Fig.3.b shows that, in the ordered state, the M-H curves at T=9.76K and T=2.0K are not different for higher fields.

The powder M-H curve at 1.7K (Fig.4) shows the magnetic moment per Gd-ion to rise rapidly at low field up to 0.4T and then slowly in the field region of $0.4 < H < 4T$. Above that, for $4T < H_{ap} < 10.3T$, the magnetization rises almost linearly as:

$$\langle g.J \rangle = 0.53 H_{ap} + 0.73 \quad (2)$$

For $H \geq H_c = 133(3)$ kOe, the saturated moment is $7.13 \mu_B$ (the expected value is 7 μ_B). The excess saturation moment ($0.13 \mu_B$) is probably due to the contaminating magnetic phases. Because of the combined effects of the magnetic impurity and the polycrystalline form, no attempt is made for estimating the spin-flop field. In this work, no correction is being carried out for diamagnetic contribution.

The resistivity (Fig.5) reveals a metallic behavior down to 30K. For $30 < T < T_1$, it reveals a temperature independent features. Below T_1, an anomalous drop in the resistivity is observed. The inset of Fig.5 demonstrates the relation between the

normalized magnetic resistivity $\Delta\rho$ and the sublatice magnetization that was measured by the Mossbauer spectroscopy [15] where M is proportional to the effective hyperfine field: $M \propto H_{eff}$. Let us assume in this case the validity of the Molecular field (MF) relations wherein $\Delta\rho(T)$ is connected to the thermally averaged Gd moment $\langle J \rangle$ as [17]:

$$\Delta\rho(T)=\{\rho(T)-\rho_0\}/\rho_0 \propto -\langle J\rangle^2 \propto -H^2_{eff} \qquad (3)$$

where ρ denotes the incoherent magnetic scattering;. $\rho = (\rho_{tot} - \rho_{ph} - \rho_{res})$ and ρ_0 is the high-T paramagnetic resistivity. The inset shows that while $-H^2_{eff}$ drops fast below T_N and slowly afterwards, the $\Delta\rho(T)$ drops with a much slower rate. No doubt, the trend is similar, however, the fact that $\Delta\rho(T)$ is not scaling well with $\langle J\rangle^2$ implies that MF approximation is not applicable for this compound. This agrees with the conclusion of the Mossbauer spectroscopy that the M-T curves can not be fitted to a MF S=7/2 Brillouin function.

Discussion

As a first approximation, let us assume that the low-T magnetic phase of $GdNi_2B_2C$ is a weak-anisotropic Heisenberg AFM. Then, MF theory expresses the magnetization isotherm (H along the easy axis) as follows [18,19]:-

$$M/M_S = H_{ap}/(2H_{ex}-H_a) \approx H_{ap}/(2H_{ex}) \qquad 4.a$$

$$H_{sat} = (2H_{ex}-H_a) \quad \approx 2H_{ex} \qquad 4.b$$

$$H_{sf} = \sqrt{(2H_aH_{ex}-H_a^2)} \qquad 4.c$$

where, H_{ex}, H_a, H_{sat} and H_{sf} are respectively the exchange field, the anisotropy field ($<< 2H_{ex}$), the saturation field and the spin-flop field. M_S is the sublattice

magnetization (½Ngμ_BJ). Although these relations are valid only for single crystal, we try below to apply them to a polycrystalline sample so as to obtain a qualitative understanding of the overall magnetic features. We will also ignore the further complication of the possible instability of the AFM ground state against a helical state at low-T [13]. Then, the qualitative features of Fig.4 can be described as follows: the external field first flops the spins to the perpendicular direction and then for higher field works to align them parallel to the field against the AFM exchange couplings. Complete moment saturation is achieved only when the exchange field is being completely counterbalanced i.e. $H_{ap} = H_{sat} = 133(3)$ kOe . The analysis of Fig.4 according to Eqs.4 shows that (i) Eq.2 fits the quasi-linear behavior of the M-H curves over a wide field range $4T<H_{ap}<10.3T$ and (ii) the value calculated from the slope of Eq.2 gives a value close to the $2H_{ex}$ and so confirms Eq.4.b i.e. $2H_{ex} = H_{sat} = 133$kOe. Moreover, Eq.(4.c) shows that the spin-flop field $\sqrt{(2.H_a.H_{ex}-H_a^2)}$ is negligible and therefore a small applied field will flop the Gd-moment perpendicular to the field direction. Although, the validity of the MF arguments on a highly anisotropic polycrystal is questionable, these self-consistent rough calculations characterize this compound as a weak anisotropic Heisenberg antiferromagnet with strong AFM interactions.

The deviation from linear behavior in the M-H curve for H< 4T and the non-proportionality of <g.J> with H_{ap} (Eq.2, in contrast to Eq.4.a, has a y-axis intercept) are most probably due to (i) the presence of magnetic impurities or (ii) the polycrystalline form of the sample or (iii) the field-induced influence on the assumed helical arrangement. Experiments are under way to resolve this feature.

The observed ordering temperature, T_1, of the $GdNi_2B_2C$ compound is the highest among the magnetic members of the RNi_2B_2C series [3,4,14]. This is not surprising since for this series, T_1 is shown [4, 14] to scale with the de Gennes factor, $(g-1)^2J(J+1)$, and this factor is the largest for the Gd-ion.

4. CONCLUSION

The magnetism of the $GdNi_2B_2C$ compound is shown to be similar to the magnetism of the isomorphous series RNi_2B_2C (R=Tm, Er, Ho, Dy, Tb). They all share the following characteristics. Firstly, FM intraplanar interactions are relatively stronger than the AFM interplanar interactions. Secondly, the AFM order occurring at T_1 is accompanied by a characteristic field cooled and zero-field features which are interpreted as being a signature of the accompanying helical arrangement of the 4f-moments. Thirdly, another magnetic transition, at T_2 is observed and interpreted as being due to order-order phase transition: a transformation from an incommensurate spin arrangement to a commensurate antiferromagnetic state. Finally, the strong character of the intra-planar AFM interactions is manifested by the fact that only high magnetic field can completely align the 4f-moments

The absence of superconductivity in this compound is related to the fact that the available electrons at the Fermi surface are participating in the mediation of the above mentioned strong RKKY interactions and so are not available for Cooper pairing. As an estimate, MF approximates the average AFM exchange field as 67 kOe.

Acknowledgment We acknowledge the fruitful discussion and critical reading of Prof. M.A. Continentino and Dr. R.C. Thiel. Experimental help from M.B. Fontes, J.C. Mondragon and R. Pereira is gratefully acknowledged.

References

[1] R. Nagarajan, C. Mazumdar, Z. Hossein, S.K. Dhar, K.V. Golpakrishna, L.C. Gupta, C. Godart, B.D. Padalia and R. Vijayaragharan, Phys.Rev.Lett. 72(1994)274.

[2] T. Siegrist, H.W. Zandbergen, R.J. Cava, J.J. Krajewski and W. F.Peck, Nature 367 (1994) 252; H.W. Zandbergen, R.J. Cava, J.J. Krajewski, W.F. Peck, Jr., Physica C224 (1. 1994)6.

[3] R.J. Cava, H. Takagi, B. Batlogg, H.W. Zandbergrn, J.J. Krajewski, W. F. Peck, Jr, T. Siegrist, B. Batlog, R. B. van Dover, R. J. Felder, K. Mizuhashi, J.O. Lee, H. Eisaki, and S. Uchida, Nature 367 (1994) 252.

[4] H. Eisaki, T. Takagi, R.C. Cava, K. Mizuhashi, J.O. Lee, B. Batlogg, J.J. Krajewski, W.F. Peck and S. Uchida, Phys.Rev.B 50(1994)647.

[5] T.E. Grigereit, J.W. Lynn, Q. Huang, A. Santoro, R.J. Cava, J.J. Krajewski and W.F. Peck, Jr, preprint.

[6] A.I. Goldman, C. Stassis, P.C. Canfield, J. Zarestky, P. Dervenagas, B.K. Cho, D.C. Johnston and B. Sternlieb, Phys.Rev.B.

[7] R. Movshovich, M.F. Hundley, J.D. Thompson, P.C. Canfield, B.K. Cho, A.V. Chubukov, Physica C 227(1994)381.

[8] M.El Massalami, S.L. Bud'ko, B. Giordanengo, M.B. Fontes, J.C. Mondragon and E.M. Baggio-Saitovitch. to appear in M^2S proceedings, Grenoble (1994).

[9] M.El Massalami, S.L. Bud'ko, B. Giordanengo, M.B. Fontes, J.C. Mondragon and E. M. Baggio-Saitovitch, preprint.

[10] H. Michor, W. Perthod, T. Holubar, N.M. Hong and G. Hilscher, to appear in M^2S proceedings, Grenoble (1994).

[11] C.V.Tomy, L.J. Chang, G. Balakrishnan and D.McK. Paul ;to appear in M^2S proceedings, Grenoble (1994)

[12] H. Schmidt and H.F. Braun preprint

[13] M.El Massalami, E .M. Baggio-Saitovitch, preprint.

[14] M.El Massalami, S.L. Bud'ko, B. Giordanengo and E.M. Baggio-Saitovitch, submitted to Physica C.

[15] F.M. Mulder, J.V.V.J.Brabers, R.C. Thiel, K.H.J.Buschow,F.R.de Boer, to appear in J. Alloys and Compounds.

[16] P. C. Canfield, B. K Cho, D. C. Johnston, D. K. Finemore, M. F. Hundley, Physica C 230 (1994) 397.

[17] B. Coqblin , The Electronic Structure of Rare-Earth Metal and Alloys: the Magnetic Heavy Rare-Earth (Acadamic Press, London, 1977).

[18] J.S. Smart, EffectiveField Theories of Magnetism ,(W.B.Saunders Company,1966) p.101.

[19] R.L. Carlin and A.J. van Duyneveldt, in Magnetic Propeties of Transition Metal Compounds, (Springer-Verlag,N.Y.,1978) p.184;

Figures captions:-

Fig.1 Room temperature Cu-K_α diffractogram for $GdNi_2B_2C$. The continuous line is a Rietveld-fit to the (dotted) experimental point. The space group and starting parameters are taken from Ref.[2]. z(B) denotes the Boron position parameter. The arrows shows the strong peak of the impurity phase identified as GdNiBC.

Fig.2 Magnetic properties of the $GdNi_2B_2C$ compound showing the Field Cooled (FC) and the Zero-Field Cooled (ZFC) M-T curves at H=10 Oe. The inset shows the reciprocal dc susceptibility χ_{dc}. The C-W fit gives $\chi = 7.946/(T-2.74K)$.

Fig.3. Magnetization isotherm for the $GdNi_2B_2C$ compound. (a) M-(H/T) curves illustrating the difference between the ordered and the paramagnetic phases (see text) (b) M-H curves for different temperatures .

Fig.4 (*Bottom*) The M-H curve at 1.7K for the $GdNi_2B_2C$ compound. The continuous line is a fit to the Molecular field predictions for a weakly Heisenberg antiferromagnet (see text). (*Top*) An expansion of the low-field region.

Fig.5. Resisitivity versus temperature for the polycrystalline $GdNi_2B_2C$ compound. The values are normalized to the resistivity value at room temperature. The inset shows the influence of the magnetic order on the resistivity below T_1; the continuous line is the square of the sublattice magnetization as given by Mossbauer Spectroscopy ($M(T) \propto H_{eff}(T)$) [Ref.15]

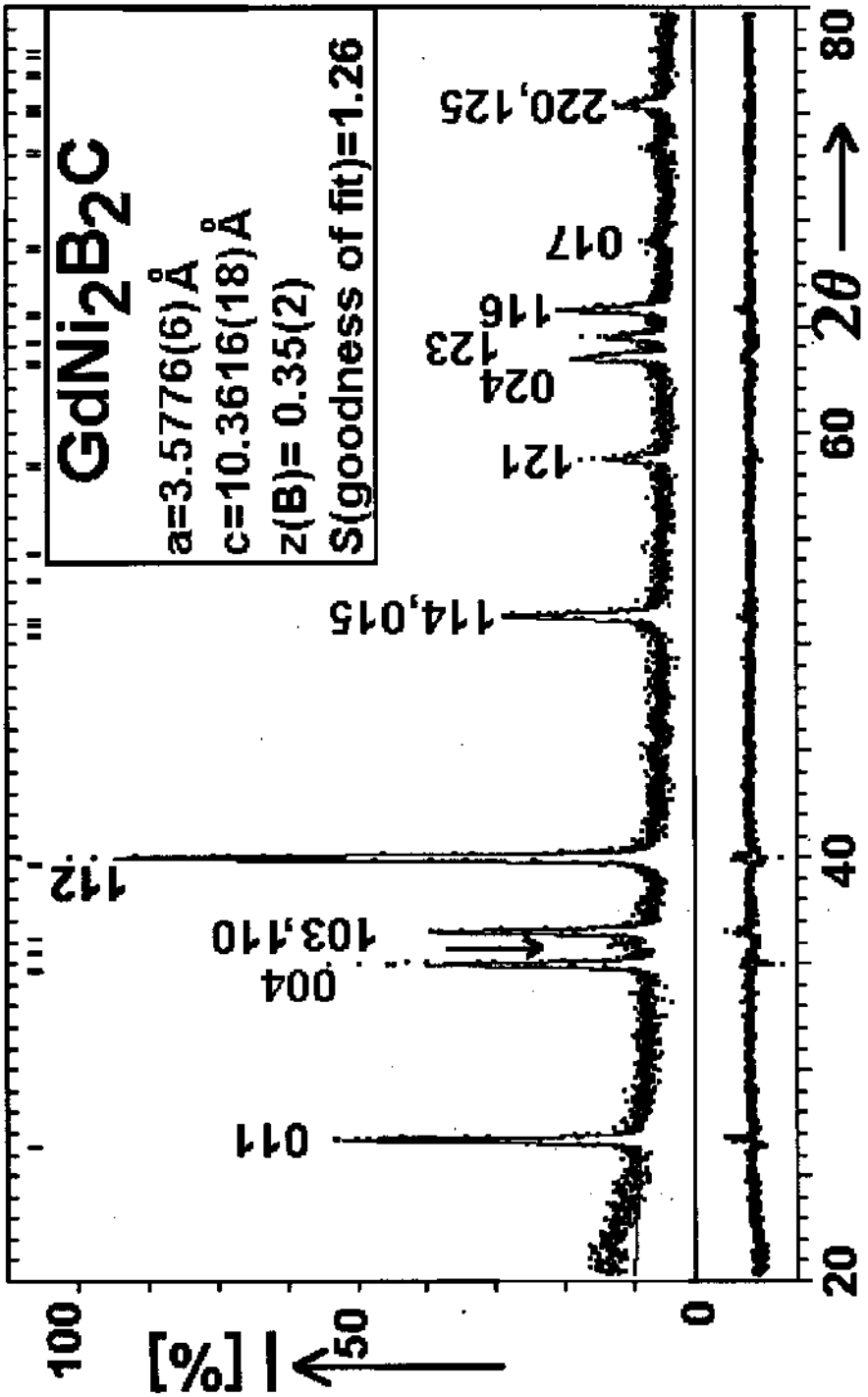
GdNi2B2C
a=3.5776(6)Å
c=10.3616(18)Å
z(B)= 0.35(2)
S(goodness of fit)=1.26
011
004
103,110
112
114,015
121
024
123
116
017
220,125
100
50
0
[%]
20
40
60
80
2θ

Fig.1

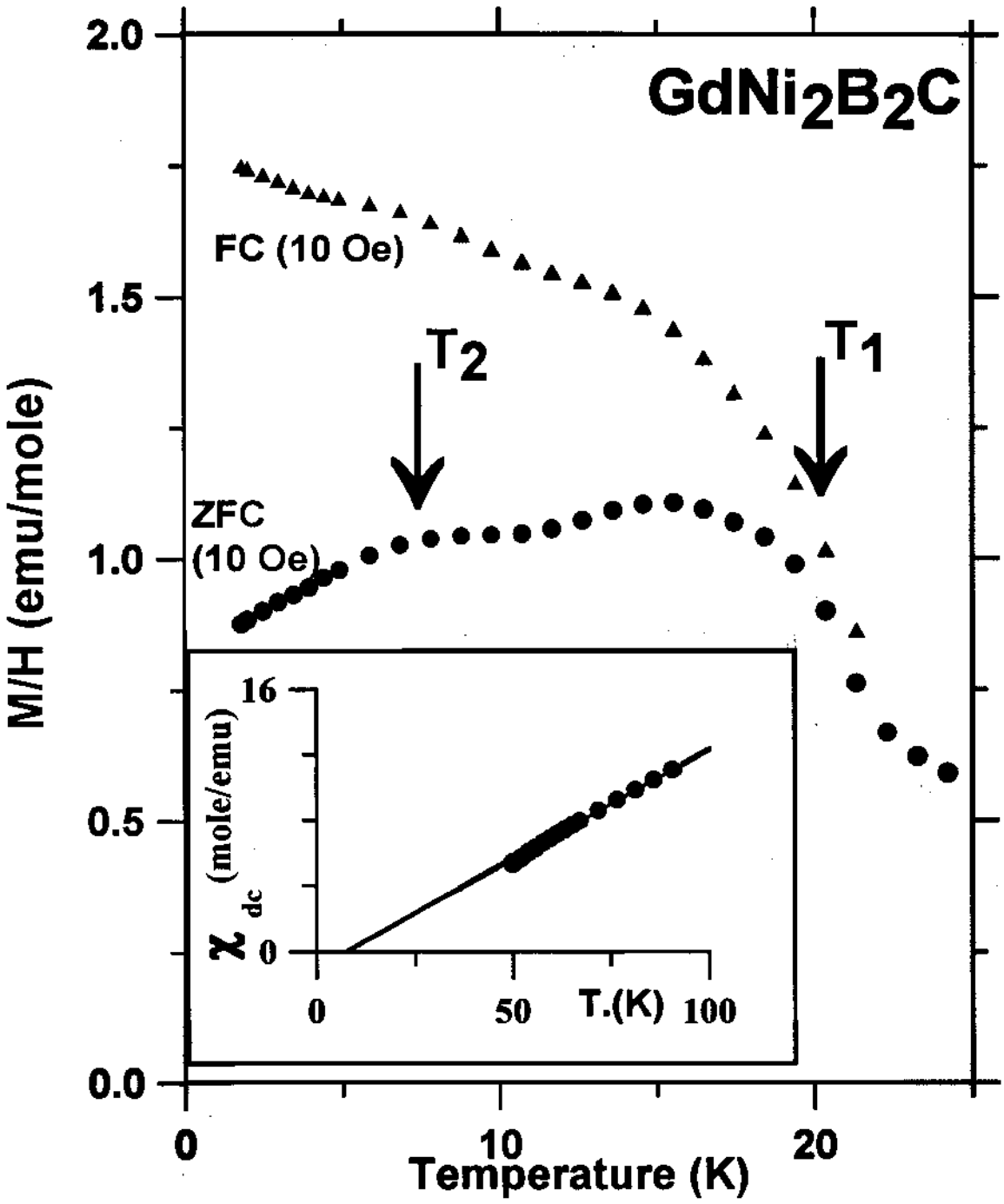
GdNi2B2C
FC (10 Oe)
ZFC
(10 Oe)
T2
T1
M/H (emu/mole)
Temperature (K)
2.0
1.5
1.0
0.5
0.0
0
10
20
χ dc (mole/emu)
16
0
0
50
T.(K)
100

Fig.2.

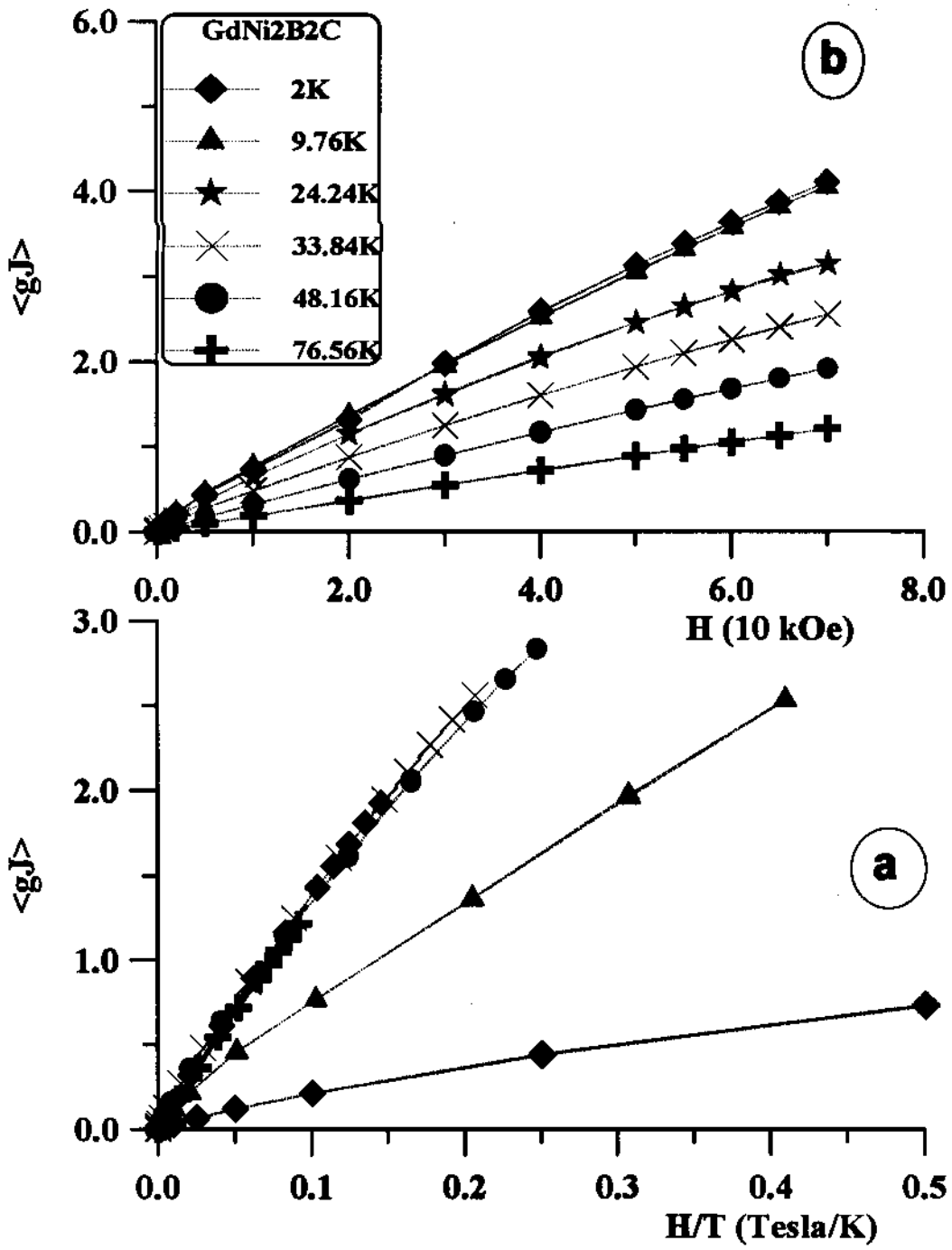
GdNi2B2C
2K
9.76K
24.24K
33.84K
48.16K
76.56K
b
<gJ>
H (10 kOe)
a
<gJ>
H/T (Tesla/K)

Fig.3

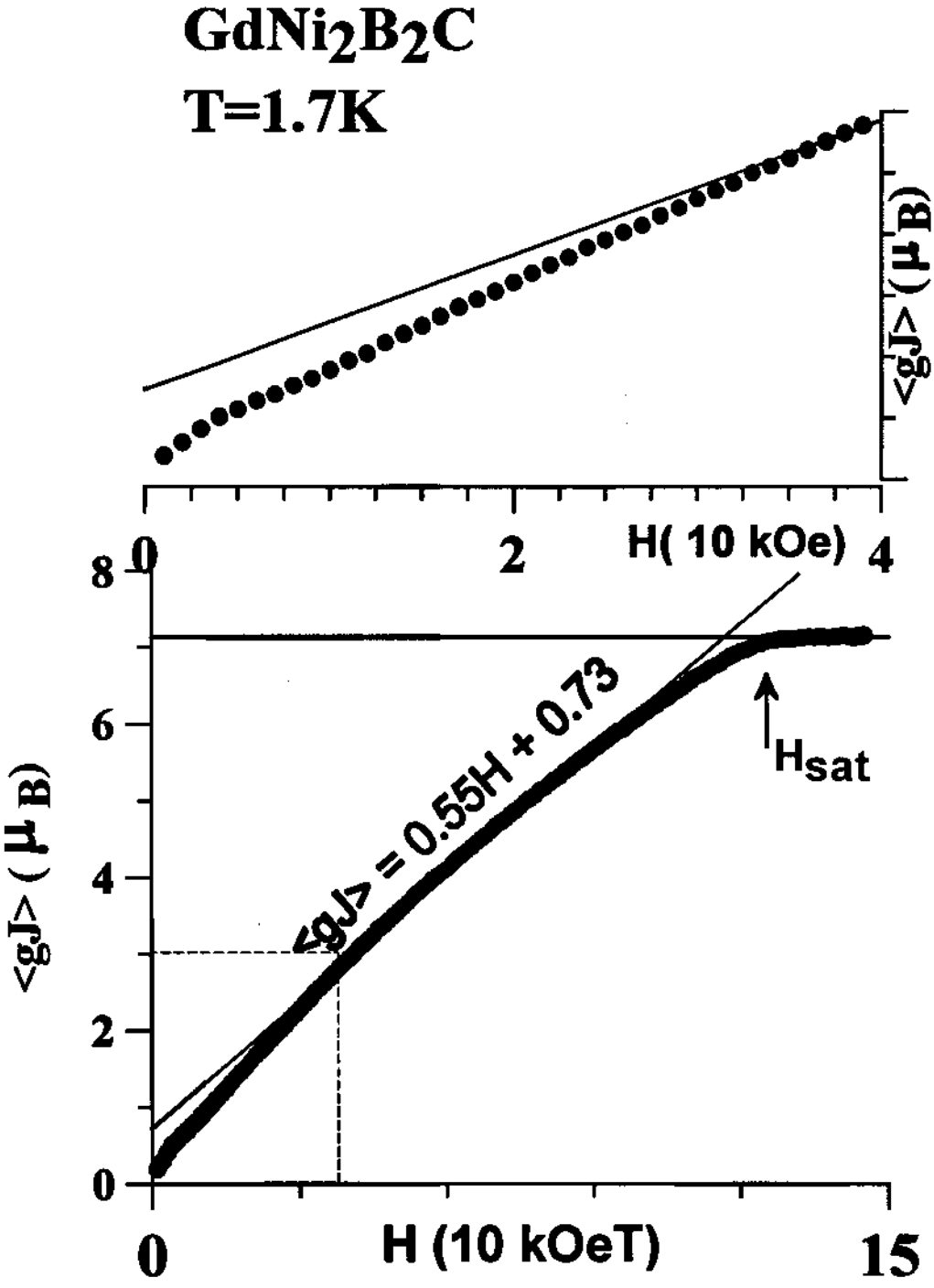
GdNi2B2C
T=1.7K
<gJ> (μB)
0
2
H(10 kOe)
4
8
6
4
2
0
<gJ> = 0.55H + 0.73
Hsat
<gJ> (μB)
0
H (10 kOeT)
15

Fig.4

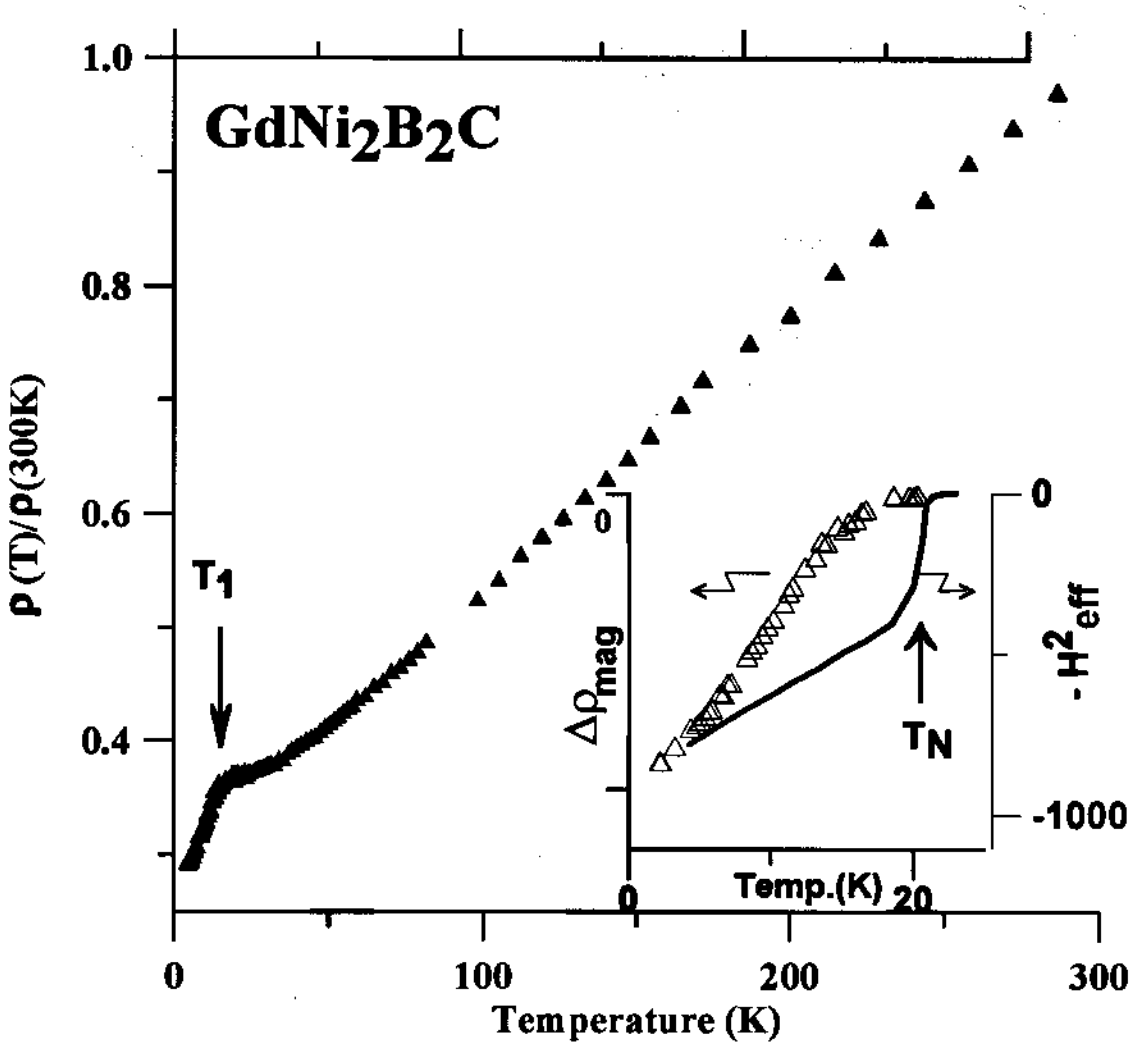
GdNi2B2C
ρ (T)/ρ(300K)
1.0
0.8
0.6
0.4
T1
0
100
200
300
Temperature (K)
Δρmag
0
0
Temp.(K)
20
TN
0
-1000
- H2eff

Fig.5